COMPUTER ASSISTED SURGERY
2019, VOL. 24, NO. S1, 96–104
https://doi.org/10.1080/24699322.2018.1557893

Taylor & Francis
Taylor & Francis Group

RESEARCH ARTICLE

OPEN ACCESS Check for updates

Experimental study on the detection of cerebral hemorrhage in rabbits based on broadband antenna technology

Haisheng Zhang*, Mingsheng Chen*, Gui Jin, Jia Xu and Mingxin Qin

Department of Biomedical Engineering, Army Medical University, Chongqing, China

ABSTRACT

Hematoma enlargement often occurs in patients with spontaneous intracerebral hemorrhage (ICH), so it is necessary to monitor the amount of intracranial hemorrhage in patients after admission. At present, the commonly used intracranial pressure (ICP) method has the disadvantages of trauma and infection, and the Computer Tomography (CT) method cannot achieve continuous monitoring. So it is urgent to develop a non-contact and non-invasive method for continuous monitoring of cerebral hemorrhage. The dielectric properties of blood are different from those of brain tissue, so the hematoma will affect the amplitude and phase of the electromagnetic waves passing through the head. A microstrip antenna was designed to construct the detection system for cerebral hemorrhage. Based on the animal model of acute cerebral hemorrhage, the detecting experiment was carried out on thirteen rabbits. Each rabbit had three bleeding states: 1, 2, and 3 ml, which represented the severity of cerebral hemorrhage. According to the measured data of high dimension and small sample, the support vector machine (SVM) algorithm was used to assess the severity of cerebral hemorrhage. According to simulation results, the antenna's forward radiation was 5 dB larger than the backward radiation, which ensured the antenna being not affected by external signals during the measurement. According to test results, the −10 dB workband of the antenna was 1.55–2.05 GHz and the frequency range of the transmission parameters S_{21} above −30 dB is 1.2 − 3 GHz. In the animal experiment, the phase difference of Transmission coefficient S_{21} was gradually increased with the increase of bleeding volume. Through the classification of 39 bleeding states of the 13 rabbits, the total accuracy was about 77%. Through animal experiments, the feasibility of detection method has been proved. But the classification accuracy need to be further improved. The detection system is based on broadband antenna has the potential to realize non-contact, non-invasive and continuous monitoring for cerebral hemorrhage.

Abbreviations: ICP: intracranial pressure; CT: computer tomography; SVM: support vector machine; TCDU: transcranial doppler Ultrasonography; NIRS: near-infrared spectroscopy; EIT: electrical impedance tomography; HFSS: high frequency structure simulator

KEYWORDS

Cerebral hemorrhage; hematoma enlargement; dielectric properties; broadband antenna; microwave technique; support vector machine; classification

Background

Cerebral hemorrhage refers to the bleeding caused by vascular rupture in the brain parenchyma, which has the characteristics of high incidence, high mortality and high morbidity [1]. Clinical studies have shown that cerebral hemorrhage is gradually aggravated, the hematoma often expands rapidly within a few hours [2], but sometimes this process lasts for several days. According to continuous CT examination of 204 patients with acute cerebral hemorrhage [3], 41 cases of hematoma expansion appear in the CT review. The most common hematoma enlargement occur within 6 hours, 15% of all occur in 6–12 hours, and 6% of all occurred within 12–24 hours, the hematoma of patients with coagulation disorders even expanded within a few days [4]. For patients with cerebral hemorrhage, hematoma enlargement is a common clinical phenomenon, which seriously threatens patient's life and prognosis [5]. So real-time monitoring of hematoma and timely clinical intervention is the key to successful treatment of patients with cerebral hemorrhage.

At present, the most commonly used monitoring method for cerebral hemorrhage is ICP [6]. However, ICP methods need to put the pressure sensor into the skull, which may lead to infection. In addition, there is

CONTACT Haisheng Zhang hsh_zhang@163.com Department of Biomedical Engineering, Army Medical University, Chongqing, China
*Haisheng zhang and Mingsheng Chen are co-frst authors.

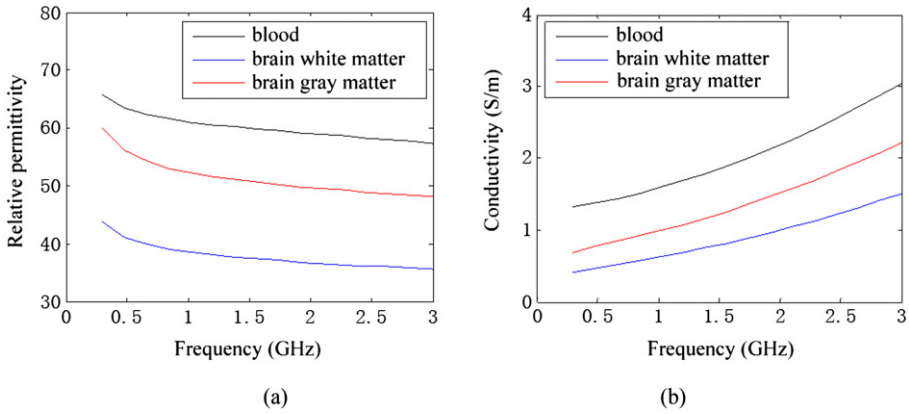

Figure 1. Relative permittivity and conductivity of blood, brain white matter and brain grey matter: (a) relative permittivity; (b) conductivity.

a lag of intracranial pressure rise compared to hematoma enlargement. CT can be used in the diagnosis of cerebral hemorrhage [7], but because of radioactivity, it is not suitable for the continuous monitoring. Therefore, it is urgent to develop a non-contact and non-invasive method for continuous monitoring of cerebral hemorrhage.

Several technologies have been researched with the aim of developing a non-invasive system that can detect early cerebral hemorrhage. Transcranial Doppler Ultrasonography (TCDU) can be used for continuous monitoring [8], but it has high requirements for the operator's level, and cannot quantify the severity of cerebral hemorrhage. Near-infrared spectroscopy (NIRS) has been proposed as a possible technology to estimate the intracranial hematoma [9,10]. But it is difficult to detect the hematoma accurately when the bleeding volume is small or the position is deep. Electrical impedance tomography (EIT) has been reported to detect cerebral hemorrhage in an animal model [11,12]. But it needs to be contacted to the scalp, and the high resistivity of the skull seriously affects the image quality.

Magnetic induction phase shift (MIPS) is a developing method of non-contact cerebral hemorrhage monitoring [13].Our experimental group had carried out a large number of rabbit brain hemorrhage monitoring experiments base on MIPS method [14]. It was found that the MIPS did reflect the severity of cerebral hemorrhage. But because the MIPS method uses the phase shift of the single frequency point, the test results are greatly affected by individual differences of experimental animals. The coil configuration of the MIPS method determines that this method cannot be used for wideband measurements.

Microwave propagation in human tissues has an advantage over both impedance and ultrasound via the easy penetration of the human skull. This is the fundamental basis for the present effort. In this paper, microwave technique was used to detect the early enlargement of hematoma in cerebral hemorrhage. According to the work of Gabriel et al. [15], the dielectric properties of blood and brain tissue is different, which provides the possibility to identify and monitor hemorrhagic stroke [16].

The objectives of this study were, the first, to analyze the of hemorrhage detection principle through simulation experiment; the second– to design the microstrip antenna for cerebral hemorrhage detection system; the third – to carry out experiments on animals; the fourth – to use the method of the support vector machine to assess the severity of cerebral hemorrhage.

Method

Detection principle

According to the work of Gabriel et al. [15], the dielectric properties of blood, brain white matter and brain grey matter in the frequency range of 0.3–3 GHz are shown in Figure 1. It is clearly shown that the relative permittivity and conductivity of blood are different from brain white matter and brain gray matter. This provides the basis for detecting the enlargement of hematoma. When the electromagnetic waves travel through the head, its amplitude and phase will be affected by the dielectric properties of the brain. With the enlargement of hematoma, the transmission and reflection of microwave signal will change, and these changes will be captured by antennas, then the hematoma size will be inferred from the changes.

A simulation experiment was designed in the software HFSS to analyze how the change of dielectric properties affects the transmission of electromagnetic

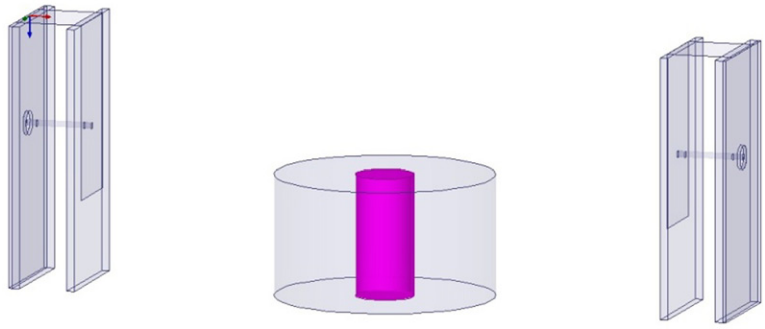

Figure 2. Simulation model of cerebral hemorrhage.

waves. The simulation model is shown in Figure 2. The transmitting antenna and the receiving antenna are located on both sides of the model, and two cylinders are arranged in the middle to simulate the biological tissue. The radius and height of outer cylinder are 22.5 and 25 mm, respectively, and the dielectric properties are $\varepsilon_r = 36.9$, $\sigma = 0.94S/\mathrm{m}$ at 1.86 GHz (which is the center frequency of antenna), it is used to simulate brain grey matter. The radius and height of outer cylinder are 6 and 25 mm, respectively, and the dielectric properties are $\varepsilon_r = 59.3$, $\sigma = 2.09S/m$ at 1.86 GHz, it is used to simulate hematoma. The whole model simulates the situation of hematoma in the brain grey matter. In the experiment, the transmitting antenna is on the left side and the receiving antenna is on the right side.

The HFSS software adopts adaptive meshing technology for the simulation model, and the model is divided into tetrahedral elements. The initial edge length of the tetrahedron is determined by the center frequency of 1.86 GHz. The mesh is then refined according to the calculation error ΔS, until the error satisfies the convergence condition. The convergence condition of this simulation adopts the default setting $\Delta S < 0.02$. In fact, the calculation error $\Delta S = 0.011$ is achieved after five iterations in the simulation. This simulation model uses radiation boundary condition to simulate the antenna in free space. The same settings are used in other simulations in this article.

In the electromagnetic theory, the Poynting vector ($\vec{S} = \vec{E} \times \vec{H}$) reflects the energy propagation of electromagnetic field, it represents the volume and direction of energy flow density. So by observing the Poynting vector, we can obtain the transmission characteristics of the microwave signal.

The simulation experiment results are shown in Figure 3. Figure 3(a) shows the propagation direction of the Poynting vector with only outer cylinder at frequency 1.86 GHz, Figure 3(b) shows the propagation direction when both cylinders exist. By comparing the two Figure(3(a,b)) we found that, (1) the insertion of the inner cylinder significantly changes the transmission path of the electromagnetic energy, it will change the phase of the transmission coefficient; (2) the relative permittivity of the inner cylinder is higher than that of the outer cylinder, so the electromagnetic energy is focused in the inner cylinder, it will change the amplitude of the transmission coefficient. The above experiment means that, the amplitude and phase of the transmission coefficient will change when the hematoma appears in the brain tissue.

Experimental system

As shown in Figure 4, the microwave-based cerebral hemorrhage monitoring system was composed of a vector network analyzer (Agilent E5061B), a transmitting antenna and a receiving antenna. The transmitting antenna and receiving antenna were connected with the two ports of the vector network analyzer respectively. The signal transmission coefficient S_{21} between the transmitting antenna and the receiving antenna was measured in the experiment.

The transmitting antenna was exactly the same as the receiving antenna. In order to improve the performance of the system, the following principles were taken into account during the antenna design: (1) the antenna near-field radiation beam should cover the entire brain, and in order to avoid external interference, the beam should be only in one direction; (2) the working bandwidth of the antenna should be wide enough to extract more information from the brain; (3) the area of the antenna should be as small as possible so that it could be easily integrated into the detection system, and it was conducive to increase the number of antennas for next generation systems. Considering the above objectives, this paper designed a microstrip antenna with side short wall as the detection antenna. The parameters of the antenna were optimized in the simulation software HFSS. As shown

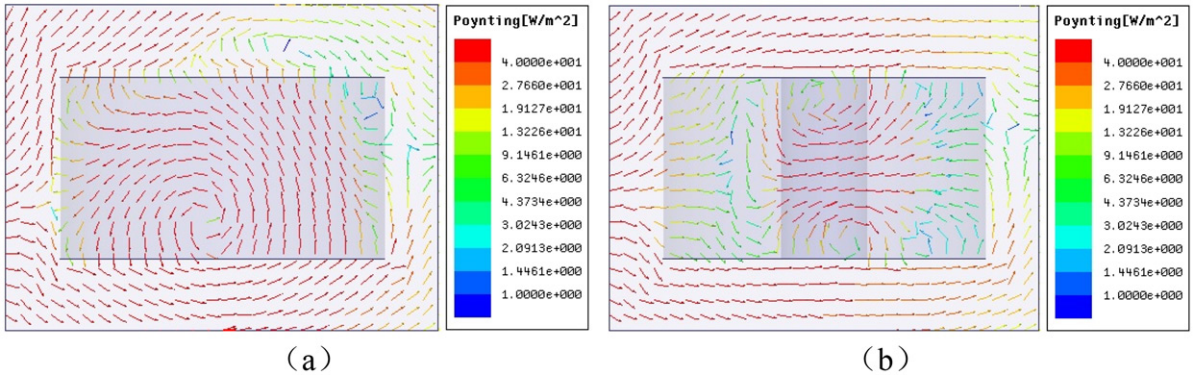

Figure 3. Poynting vector in model of cerebral hemorrhage: (a) separate grey matter cylinder; (b) grey matter and blood cylinders.

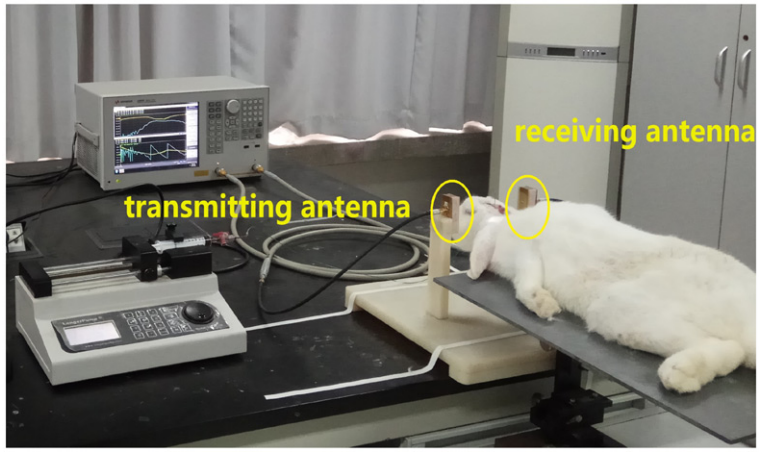

Figure 4. Experimental system of rabbit cerebral hemorrhage.

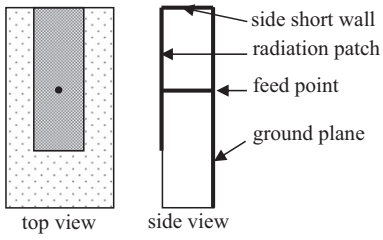

Figure 5. Antenna structure.

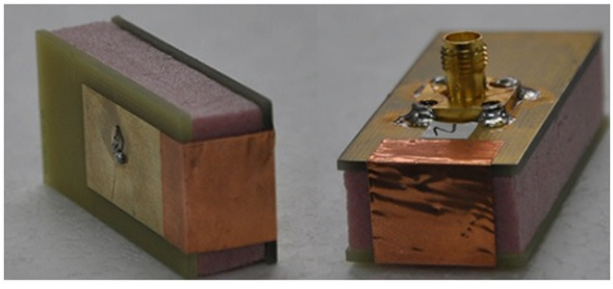

Figure 6. Antenna prototype.

in Figure 5, the overall length, width and height of the antenna are 49 mm × 24 mm × 13.2 mm. The radiation layer and the ground layer are made of printed circuit board with a thickness of 1.6 mm. The space between the radiation layer and the ground layer is filled with high density foam with a thickness of 10 mm. The size of the radiation patch and ground plane are 37 mm ×16 mm and 49 mm × 24 mm respectively. The side short wall is made of self-adhesive copper foil with a width of 16 mm. The feed point is located in the middle of the antenna, 25 mm from the side wall. Due to the use of side short wall, the size of the antenna is relatively small, and because of the thick dielectric layer, the workband of the antenna is wide. The prototype of the antenna is shown in Figure 6.

The head is in the near-field of the antenna during the measurement, so we are concerned about the near-field radiation of the antenna. The software HFSS was used to simulate the near field of the antenna. Figure 7(a) describes the relative position of the antenna and the coordinate system, the origin of the coordinate system is located at the center of the antenna ground plane. Figure 7(b) shows the 3 D electric field beam of the antenna on the spherical surface with a radius of 100 mm (which was obtained at

$$S_{\text{energy\_density}} = E^2 / 377\Omega \quad (1)$$

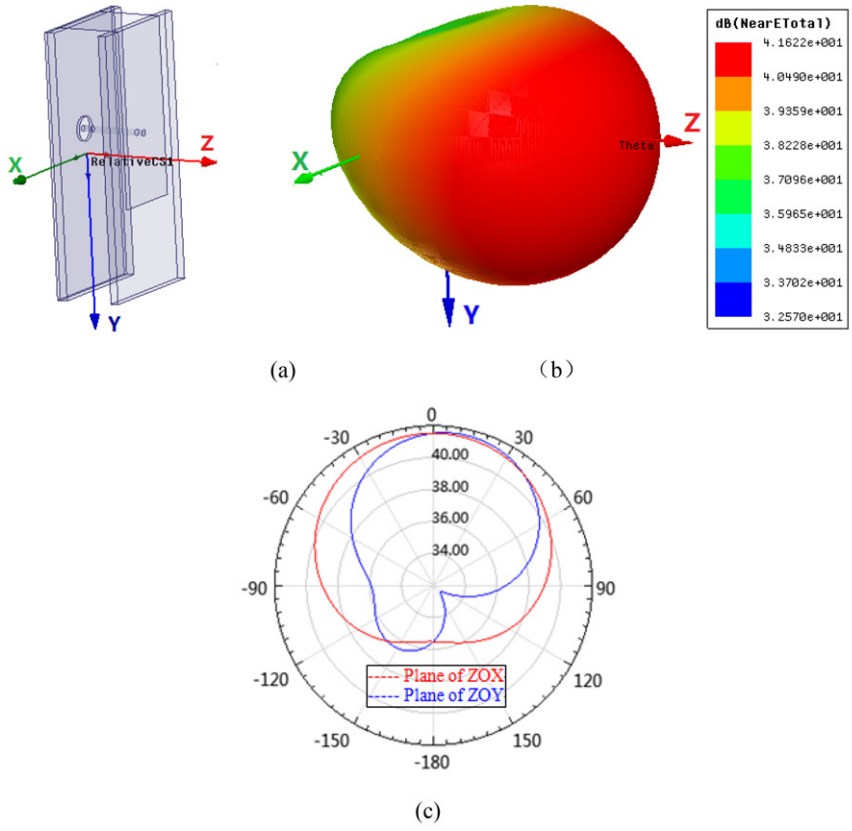

Figure 7. Antenna near field simulation pattern (1.86 GHz): (a) coordinate origin position, (b) 3D electric field pattern (r = 100 mm), (c) plane electric field pattern (r = 100 mm).

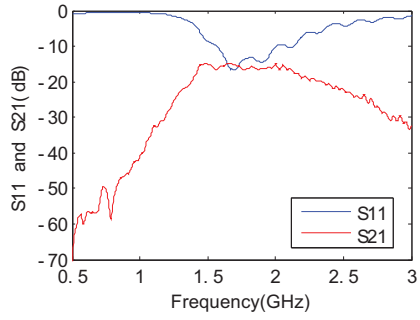

Figure 8. System working band.

antenna's center frequency 1.86 GHz). It can be seen that the radiation beam of the antenna is in the normal direction of the patch, it shows good unidirectional. Figure 7(c) shows the electric field beam on ZOX plane and ZOY plane (r = 100 mm), It can be seen that the forward radiation is 5 dB larger than the backward radiation, which ensures that the antenna is not affected by external signals during the measurement.

The maximum electric field is 41.6 dB (120.2 V/m), which is obtained under the excitation power of 1 W. In the cerebral hemorrhage monitoring system, the excitation power of the vector network analyzer is 1mW, so the electric field value is about 3.80V/m according to the conversion ratio ($120.2/\sqrt{1000}$). According to the formula (1), the electric field value is converted into energy density 0.00383 mW/cm^2, which is much smaller than the permitted value 6.2 mW/cm^2 of the IEEE standard at this frequency [17]. So if the antenna is used on the human head, it also meets the electromagnetic radiation standard.

$$S_{\text{energy\_density}} = E^2/377\Omega \quad (1)$$

The working band of the antenna was measured by vector network analyzer. The test state is shown in Figure 4 (without rabbit), two antennas are placed opposite with a distance of 13 cm. The results are shown in Figure 8. The −10 dB working band of the single antenna reflection coefficient S_{11} is 1.55–2.05 GHz. The frequency range of the transmission parameters S_{21} above −30 dB is 1.2–3 GHz. In animal experiments it is found that, in this frequency range, the S_{21} parameter has a significant response to the hematoma, so this range is defined as the system working band.

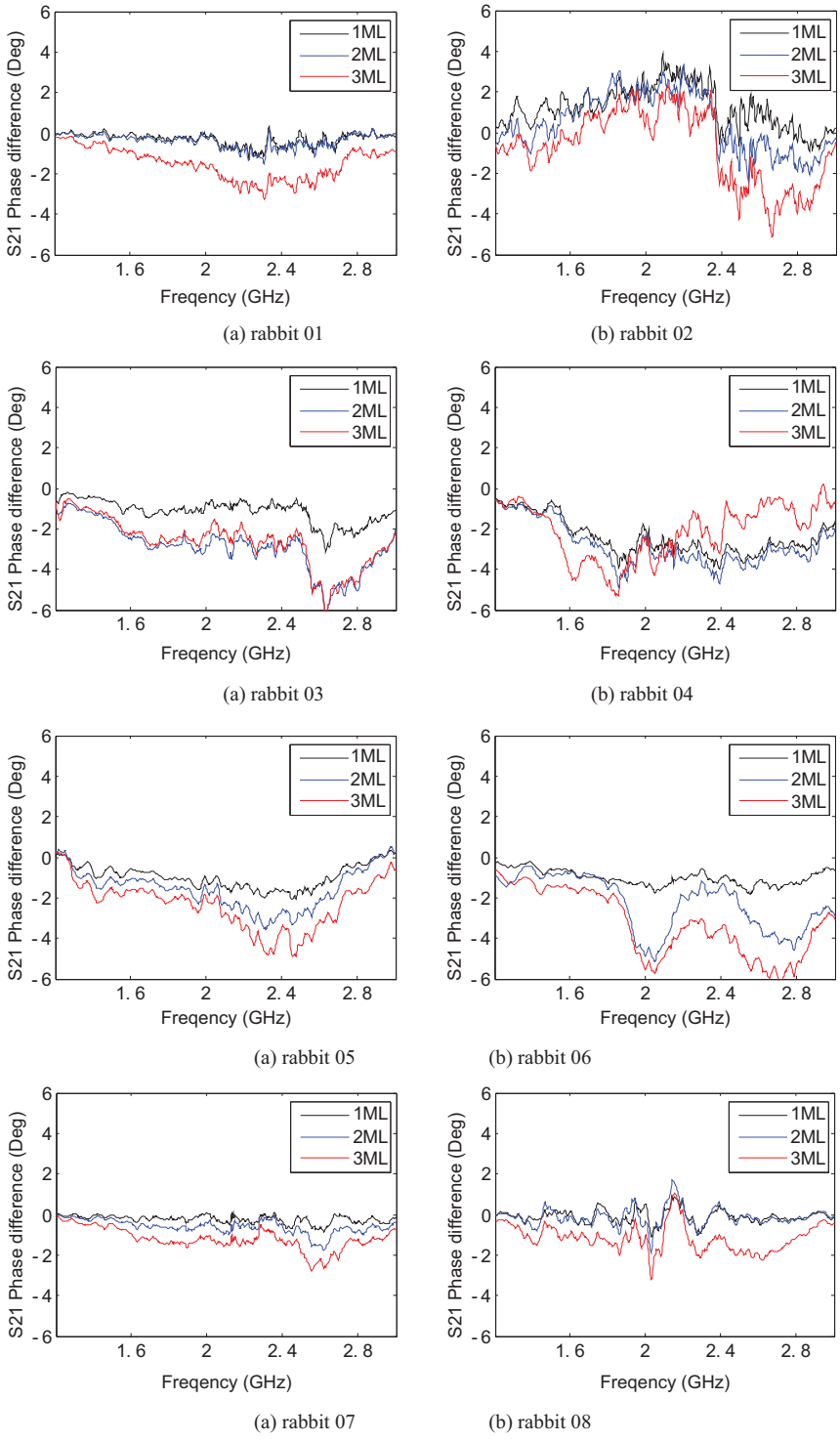

Figure 9. Phase difference of S_{21}.

Experimental design

According to the work of Chung et al. [18], most of the cerebral hemorrhages occur in the basal ganglia and the inner capsule, and the bleeding in basal ganglia often invades into the internal capsule. Therefore, experiments of inner capsule hemorrhage on rabbits were carried out in thisstudy. The experimental platform of cerebral hemorrhage in rabbits is shown in Figure 4, and the experimental steps are as follows:

1. Thirteen rabbits (2.5 ± 0.3kg) were selected and anesthetized by injecting urethane (25%, 5ml/kg) via ear vein.

Table 1. Classification results of the bleeding states.

Number	Classification results of the bleeding 1ml	Classification results of the bleeding 2ml	Classification results of the bleeding 3ml
1	1	1	3
2	1	2	3
3	1	3	3
4	2	2	3
5	1	2	3
6	1	3	3
7	1	2	2
8	1	1	1
9	1	2	3
10	1	2	3
11	1	2	2
12	1	2	3
13	2	2	3

2. In the case of complete anesthesia, a total of 4ml blood was extracted from the femoral vein of the rabbit, and stored in heparin anticoagulant tube.
3. Take the skull 'cross stitch' intersection as the origin, the drill position, which was 6 mm to the right of the coronal suture and 1mm posterior to the sagittal suture, was determined. A needle tube with a diameter of 0.7 mm was inserted into the skull to a depth of 13 mm. Dental cement was used to seal the gap between the tube and hole, it played a role in fixing the needle and preventing leakage.
4. Then the 3ml blood collected before was injected into the brain at the rate of 1 ml/min through an electronic injection pump. The injection was completed step by step with an increment of 1ml.
5. The experimental data of 0, 1, 2 and 3 ml were recorded in the experiment, and the data processing was completed in software Matlab.

It should be noted that in order to prevent the injected blood from being diffused or metabolized, the injection rate is as fast as 1 ml/min. This simplifies the experimental variable parameters and the experimental model is more accurate.

Evaluation method for severity of cerebral hemorrhage

In animal experiments it was found that, the transmission parameter S_{21} had a negative relationship with the amount of the injection. The S_{21} phase was gradually decreased with the increase of injection volume. So we could infer the injection volume through the change value of S_{21} parameter, which was obtained by using the S_{21} parameter of bleeding 1, 2 and 3 ml subtracting the S_{21} parameter of 0 ml.

The change value of S_{21} is wideband data within 1.2–3 GHz. If we set a sampling point every 5 MHz, the dimension of change value of S_{21} will be 361. For such high-dimensional data, it is not a good idea to measure the similarity and otherness by Euclidean distance because of the curse of dimensionality. Traditional statistical analysis is also not suitable for dealing with high- dimensional data. Therefore, SVM method was used to process the experimental data in this paper. SVM method was first proposed by Corinna and Vapnik in 1995 [19]. It has many unique advantages in solving small sample, nonlinear and high dimensional pattern recognition. The basic idea is to map the vector which is linearly inseparable in low dimensional space to a high dimensional feature space through the kernel function. Then the images of the original data have a linear relationship in the feature space. With the optimal classification surface and the optimal decision function constructed, the classification is realized in the high dimensional feature space.

The SVM algorithm needs to divide the experimental data into two parts, one is training group, and the other one is test group. The training group is used to construct the classification function, and the test group is used to test the accuracy of the classification function. In this paper, the data of training group is the phase change value of S_{21} within 1.2–3 GHz, which corresponds three bleeding state: 1, 2, and 3 ml. So it is a multi-class classification problem, we need to expand the binary classification SVM method to multi-classification SVM method. For any two kinds of samples, a binary classifier will be generated, and finally we get three binary classifiers. For the unknown sample in the test group, all three classifiers are used for classification, and then the result appear most in the three classifiers is taken as the final result of the classification.

This paper used the LIBSVM toolkit provided by Chang and Lin [20] to analyze the data, Gauss kernel was selected as the mapping function, and the penalty parameter C used the default value.

Result

The measured data in experiment contained the magnitude and phase of the reflection coefficient S_{11} and the transmission coefficient S_{21}. In the classification analysis, it was found that the classification accuracy was the highest when the phase of S_{21} was used alone. Figure 9 shows the S_{21} phase data of 8 rabbits, the data of the other 5 rabbits are similar, so they are not shown in this paper. It should be noted that, these data is the difference volume of S_{21} phase, which is obtained by using the S_{21} phase of bleeding 1, 2 and 3 ml subtracting the S_{21} phase of 0 ml. In the

actual detection system, the change of hematoma is also reflected by the change of the measured data.

As shown in Figure 9, the phase difference of S_{21} is gradually increased with the increase of injection volume, but the detail of the change is not the same. The frequency corresponds to the maximum change is at about 2.4 GHz for rabbit 01, rabbit 05 and rabbit 07, and the frequency of the rest rabbits is not here, but still concentrated in the 1.2–3 GHz operating frequency band. Most of the S_{21} phase change values are negative except rabbit 02. This irregular data makes it impossible to classify by simple statistical analysis. This is also the reason why this paper finally used the SVM method for data analysis.

The blood injection experiment was carried out on thirteen rabbits. As the sample number is small, if they are divided into training group and test group, the classification result will be poor. So leave-one-out cross validation method was used in this paper. Specifically, each time 12 rabbits were assigned to the training group, leaving only one to the test group, and then looped 13 times for all the samples. The calculation of leave-one-out was relatively complex, but due to the high sample utilization, it was suitable for small sample situation. Through the cross validation on 13 rabbits, it was found that when the S_{21} phase was used alone as the sample data, the classification accuracy was the highest. Therefore, this paper gave the classification results of sample data with S_{21} phase alone.

In Table 1, each row is the classification results of the three bleeding states 1, 2 and 3 ml. If the classification results are 1, 2 and 3 successively, the classification is correct, otherwise it is wrong. There are 9 errors in the 39 classification results, the total accuracy is about 77%.

The classification of rabbit 5 is correct, and there are two errors in rabbit 8. Taking the two as the representative, the relationship between the S_{21} phase difference and the classification result is studied. As shown in Figure 9, the S_{21} phase difference of rabbit 5 is gradually increased with the increase of injection volume. With the injection volume increases 1 ml, the maximum phase change of S_{21} increases about 1.5 degrees. However, the phase change of rabbit 8 is smaller, after the injection of 3 ml, the maximum value is still within 2 degrees, and so the algorithm determines that the injection volume is still 1 ml.

Discussion

In the classification analysis, it was found that the classification accuracy was the highest when the phase of the transmission coefficient S_{21} was used alone. This phenomenon can be explained as follow. Firstly, for the change of dielectric properties caused by hemorrhage, the sensitivity of the phase is greater than the sensitivity of the amplitude. Secondly, the transmission coefficient S_{21} represents the electromagnetic waves that travel through the brain, and the reflection coefficient S_{11} represents the electromagnetic waves reflected by the brain. The electromagnetic wave propagation depth of S_{21} is greater, so it is more sensitive for the bleeding in deep brain.

Through the above experiments we confirm that it is feasible to detect the changes of hematoma by microwave technique. The 3 ml hematoma in rabbit brain can be detected by electromagnetic waves across the brain, and then according to the phase change of the transmission coefficient S_{21}, the volume change of the hematoma is deduced.

However, the classification accuracy is less than 77% in the analysis of the 39 bleeding state of the 13 rabbits. This current correct rate only proves its feasibility, there is still a large distance from the clinical application, and the classification accuracy needs to be further improved. By analyzing the detection data, it is found that the reason for the misclassification is in the data collection itself, not the classification algorithm, so in order to increase the classification accuracy; we need improve the quality of the experimental data first.

There are two ways to improve the quality of experimental data. Firstly, the consistency of experimental data needs to be ensured; secondly, the sensitivity of the detection system on bleeding needs to be improved.

To ensure the consistency of the experimental data means that, for the same volume of bleeding in different rabbits, the phase change of S_{21} keeps consistent as far as possible, so that the classification model based on sample learning is more accurate. The factors which affect the consistency of the experimental data contain the individual differences and position change of the rabbits in different experiments. In the future work, for the individual difference of the rabbits, we consider doing normalization for the head circumference and the body weight of the rabbits. For the position change between rabbits and antennas, we consider building a multi-channel detection system. That is, more antennas are distributed around the head, so the antenna coverage angle is wider and the sensitivity of the location is reduced. And moreover, the information extracted from the brain is more

fully. So the error caused by the position change is minimized as far as possible.

To improve the sensitivity of the detection system on bleeding means that, for different bleeding volume, the detection parameters of the system are more obvious. In this paper, the radiation antenna is designed for human head. In the future work, we consider improving the antenna by increasing the directivity of the antenna near field radiation, so the radiation beam is more concentrated on the bleeding area.

Conclusion

This paper proposed a new method based on microwave technique to detect the cerebral hemorrhage, which had the potential to develop a non-contact and non-invasive system for continuous monitoring of cerebral hemorrhage. In the data analysis, the relationship between the phase difference of S_{21} and the amount of bleeding was revealed. According to the experimental data of high dimension and small sample, the support vector machine method was used to classify the bleeding volume. Through animal experiments, the feasibility of this method had been proved. However, the classification accuracy needs to be further improved; the potential method is to improve the detection ability of the antenna and to build a multichannel detection system.

Disclosure statement

No potential conflict of interest was reported by the authors.

This paper is supported by Army Medical University Achievement Transformation Fund (No. 014XZH03) and National Natural Science Foundation of China (No. 61372065).

References

[1] Li Y, Fang W, Tao L, et al. Efficacy and safety of intravenous nimodipine administration for treatment of hypertension in patients with intracerebral hemorrhage. Neuropsychiatr Dis Treat. 2015;11:1231–1238.

[2] Broderick JP, Brott TG, Tomsick T, et al. Ultra-early evaluation of intracerebral hemorrhage. J Neurosurg. 1990;72:195–199.

[3] Kazui S, Naritomi H, Yamamoto H, et al. Enlargement of spontaneous intracerebral hemorrhage. Incidence and time course. Stroke. 1996;27:1783–1787.

[4] Cucchiara B, Messe SL, Kasner S, et al. Hematoma growth in oral anticoagulant related intracerebral hemorrhage. Stroke. 2008; 39:2993–2996.

[5] Mendelow AD, Gregson BA, Rowan EN, et al. Early surgery versus initial conservative treatment in patients with spontaneous supratentorial lobar intracerebral haematomas (STICH II): a randomised trial. Lancet. 2013; 382:397–408.

[6] Tian Y, Wang Z, Jia Y, et al. Intracranial pressure variability predicts short-term outcome after intracerebral hemorrhage: a retrospective study. J Neurol Sci. 2013; 330:38–44.

[7] Fieschi C, Carolei A, Fiorelli M, et al. Changing prognosis of primary intracerebral hemorrhage: results of a clinical and computed tomographic follow-up study of 104 patients. Stroke. 1988;19:192–195.

[8] Nakae R, Yokota H, Yoshida D, et al. Transcranial Doppler ultrasonography for diagnosis of cerebral vasospasm after aneurysmal subarachnoid hemorrhage: mean blood flow velocity ratio of the ipsilateral and contralateral middle cerebral arteries. Neurosurgery. 2011;69:876–883.

[9] Zweifel C, Castellani G, Czosnyka M, et al. Continuous assessment of cerebral autoregulation with near-infrared spectroscopy in adults after subarachnoid hemorrhage. Stroke. 2010;41:1963–1968.

[10] Zhang Y, Chan GSH, Tracy MB, et al. Cerebral near-infrared spectroscopy analysis in preterm infants with intraventricular hemorrhage. Conf Proc IEEE Eng Med Biol Soc 2011;2011:1937–1940.

[11] Xu CH, Wang L, Shi XT, et al. Real-time imaging and detection of intracranial haemorrhage by electrical impedance tomography in a piglet model. J Int Med Res. 2010; 38:1596–1604.

[12] Xu C, Dai M, You F, et al. An optimized strategy for real-time hemorrhage monitoring with electrical impedance tomography. Physiol Meas. 2011;32: 585–598.

[13] Jin G, Sun J, Qin M, et al. A special phase detector for magnetic inductive measurement of cerebral hemorrhage. Plos One. 2014;9:e97179.

[14] Pan W, Yan Q, Qin M, et al. Detection of cerebral hemorrhage in rabbits by time-difference magnetic inductive phase shift spectroscopy. Plos One. 2015;10: e0128127.

[15] Gabriel S, Lau RW, Gabriel C. The dielectric properties of biological tissues: II. Measurements in the frequency range 10 Hz to 20 GHz. Phys Med Biol. 1996; 41:2251–2269.

[16] Persson M, Fhager A, Trefna HD, et al. Microwave-based stroke diagnosis making global prehospital thrombolytic treatment possible. IEEE Trans Biomed Eng. 2014;61:2806–2817.

[17] IEEE. IEEE standard for safety levels with respect to human exposure to radiofrequency electromagnetic fields, 3 kHz to 300 GHz[J]. IEEE Std C95.1–1999, 1999.

[18] Chung C, Caplan LY, Chang H, et al. Striatocapsular haemorrhage. Brain. 2000; 123: 1850–1862.

[19] Cortes C, Vapnik V. Support-vector networks. Mach Learn. 1995; 20:273–297.

[20] Chang CC, Lin CJ. LIBSVM: A library for support vector machines. ACM Trans Intell Syst Technol. 2011; 2: 1–39.